

Upregulation of SKA3 enhances cell proliferation and correlates with poor prognosis in hepatocellular carcinoma

JIANXIN TANG^{1,2*}, JING LIU^{3*}, JINJUN LI^{1*}, ZIMING LIANG⁴, KAINING ZENG⁴,
HAIBO LI⁴, ZHENLIN ZHAO⁵, LI ZHOU⁶ and NAN JIANG¹

¹Department of Hepatic Surgery (Liver Transplantation), The Third People's Hospital of Shenzhen (The Second Affiliated Hospital of Southern University of Science and Technology), Shenzhen, Guangdong 518000;

²Department of General Surgery, Foshan Hospital Affiliated to Southern Medical University, Foshan, Guangdong 528000;

Departments of ³Infectious Diseases and ⁴Hepatic Surgery, Liver Transplant Center, The Third Affiliated Hospital of Sun Yat-sen University, Guangzhou, Guangdong 510630; ⁵Shenzhen Ruipuxun Academy for Stem Cell and

Regenerative Medicine, Shenzhen, Guangdong 518000; ⁶Department of Rehabilitation, The First Affiliated Hospital of Clinical Medicine of Guangdong Pharmaceutical University, Guangzhou, Guangdong 510000, P.R. China

Received June 2, 2020; Accepted November 23, 2020

DOI: 10.3892/or.2021.7999

Abstract. Hepatocellular carcinoma (HCC) is one of the most aggressive types of malignancy worldwide. However, the mechanism underlying its frequent recurrence remains unclear. Studies have demonstrated that spindle and kinetochore associated complex subunit 3 (SKA3) is highly expressed in colorectal and prostate cancer. The present study aimed to determine whether SKA3 could be a predictive and prognostic marker for liver cancer. SKA3 expression levels in liver cancer cell lines, liver cancer tissues, normal liver cells and non-cancerous tissues were compared at both transcriptional and translational levels. Correlation between SKA3 levels, clinicopathological characteristics and patient survival was also assessed. Gene set enrichment analysis (GSEA)

was performed to identify SKA3-associated pathways. Furthermore, SKA3 was knocked down and overexpressed in liver cancer cells, and then assessed the effect on cell proliferation, cell cycle, and tumor formation ability. Kaplan-Meier survival analysis and log-rank test were used to evaluate the association between SKA3 expression levels and prognosis. SKA3 mRNA and protein expression levels were significantly higher in liver cancer cell lines and clinical samples, compared with normal controls. Immunohistochemical analysis of 110 patients revealed that upregulation of SKA3 correlated with clinical pathological characteristics and patient survival. GSEA showed that BENPORATH_PROLIFERATION gene set signaling pathways were correlated with SKA3 expression levels. Luciferase reporter activity assay revealed that knockdown of SKA3 significantly inhibited the activity of transcription factor E2F. Downregulation of SKA3 significantly inhibited cell proliferation, cell cycle arrest in G₁-S phase and tumorigenesis both *in vitro* and *in vivo*, decreased the expression levels of cyclin D1 and phosphorylated-retinoblastoma and increased those of p21, suggesting a potential role of SKA3 in mediating tumor cell cycle and progression. SKA3 may function as an oncogene in liver cancer and may be a promising prognostic biomarker and candidate for targeted therapy.

Correspondence to: Professor Nan Jiang, Department of Hepatic Surgery (Liver Transplantation), The Third People's Hospital of Shenzhen (The Second Affiliated Hospital of Southern University of Science and Technology), 29 Bu Lan Road, Shenzhen, Guangdong 518000, P.R. China
E-mail: nijang163@163.com

Professor Li Zhou, Department of Rehabilitation, The First Affiliated Hospital of Clinical Medicine of Guangdong Pharmaceutical University, 19 Nonglinxia Road, Guangzhou, Guangdong 510000, P.R. China
E-mail: lilydoctor@163.com

*Contributed equally

Abbreviations: HCC, hepatocellular carcinoma; GSEA, gene sets enrichment analysis; RT-qPCR, reverse transcription-quantitative PCR; OD, optical density; shRNA, short hairpin RNA; 3'UTR, 3' untranslated region

Key words: spindle and kinetochore associated complex subunit 3, hepatocellular carcinoma, cell proliferation, prognosis

Introduction

Hepatocellular carcinoma (HCC) is the fifth most common cancer in the world and the third leading cause of death from cancer, with a global annual mortality of >780,000 deaths (1,2). The poor overall survival rate of patients with HCC is primarily caused by late diagnosis of the disease, which precludes therapeutic radical surgery for the majority of patients (3) because of the high potential for metastasis and recurrence. The prognosis for patients suitable for radical surgical resection is still poor (4,5). However, the molecular mechanism underlying the development and progression of liver cancer remain

largely unknown. Greater understanding of the transcriptional activation of oncogene signaling pathways and the control of cancer-associated genes may improve early diagnosis and prognosis, thus potentially decreasing adverse clinical outcomes for patients with liver cancer.

The spindle and kinetochore-associated (SKA) protein complex is essential for accurate chromosome segregation during mitosis, and comprises two copies of the SKA1, SKA2 and SKA3 proteins (6-10). SKA3, a novel kinetochore protein, may directly mediate kinetochore-microtubule interactions (8). SKA3 was first identified by screening for overexpressed genes in colorectal cancer (11,12). SKA3 is located at chromosome 13q12.11 and may be involved in malignant transformation (11-13). Overexpression of SKA3 has been implicated in breast and prostate cancer and is associated with increased aggressiveness in carcinoma (13,14). Deregulation of SKA3 increases the proliferation of colorectal cancer cells and promotes G₂/M arrest and entry into S phase of the cell division cycle (11). These findings suggested that SKA3 serves an important role in the development and progression of human malignant tumors. However, the expression pattern, clinical relevance and potential molecular mechanism of SKA3 in liver cancer are still controversial and remain to be explored.

The present study evaluated the prognostic significance of SKA3 expression in HCC using The Cancer Genome Atlas (TCGA) database. Cell cycle-associated genes and pathways that were altered in response to changes in SKA3 expression levels were further evaluated using gene sets enrichment analysis (GSEA). We analyzed the expression of SKA3 in liver cancer. Then, we specifically knocked down and overexpressed SKA3, and assessed the effect on cell proliferation, cell cycle, and tumor formation ability in liver cancer cells. Collectively, the present study revealed that SKA3 may be a potential diagnostic and prognostic marker in liver cancer and an effective target for the treatment this disease.

Materials and methods

Patients and tissue samples. The present study used paraffin-embedded HCC samples from 110 patients who underwent curative hepatectomy. Patients should fulfill the following criteria: No evidence of extrahepatic metastasis, main portal vein infiltration/thrombosis, and eligible for curative hepatectomy. Exclusion criteria for this study included: Rehepatectomy, preoperative combination with other tumors or prior history of other tumors. The samples had been clinically and histologically diagnosed at the Third Affiliated Hospital of Sun Yat-sen University (Guangzhou, China) between January 2011 and December 2012. A total of 10 HCC and 3 normal tissue samples were frozen and stored in liquid nitrogen and these tissues to investigate the mRNA and protein levels of SKA3. A total of three normal liver specimens obtained from the edge of the liver were used to isolate normal primary human hepatocytes. The HCC samples were obtained from patients: 99 (90%) men and 11 (10%) women. The median age of the patients was 54 years (range, 31-76 years). The patients were followed up from 1-77 months, with a median of 23 months. Clinicopathological information is summarized in Table I. All clinical specimens were obtained with informed consent and the study was approved by the Clinical Research

Ethics Committee of the Third Affiliated Hospital of Sun Yat-sen University. Informed written consent was obtained from all patients. Tumor stages were determined according to the HCC TNM staging system of the 8th American Joint Committee on Cancer (AJCC) in January 2018 (15).

Cell lines and transfection. Hep3B, Huh7, SK-Hep1, HepG2, MHCC97-H, MHCC97-L, SNU-387 and SNU-475 liver cancer cells were obtained from the Cell Bank of Shanghai Institute of Biology, Chinese Academy of Science (Shanghai, China). Normal primary human hepatocytes were isolated from liver specimens using a standardized two-step collagenase perfusion technique (16,17). High yield and high activity normal liver cells were obtained. All cells were cultured in DMEM, supplemented with 1% penicillin-streptomycin (both Invitrogen; Thermo Fisher Scientific, Inc.) and 10% FBS (HyClone; GE Healthcare Life Sciences) at 37°C with 5% CO₂. Cells were sub-cultured every 1-2 days to maintain logarithmic growth. Huh7 and HepG2 were transfected with short hairpin (sh)RNA against SKA3 to knock down SKA3, and lentivirus overexpressing vector to increase the expression of SKA3. Vector and non-specific scramble shRNA were used as negative controls. The plasmids for expression of SKA3, SKA3-specific shRNA, and their relevant lentiviruses were obtained from Shanghai GeneChem, Co., Ltd. The cells were incubated in a humidified 5% CO₂ atmosphere for 24 h at 37°C. Finally, the diluted virus was replaced with fresh medium and incubated for another 48 h under the same conditions. Subsequently, the transfection efficiency was examined by western blotting. Liver cancer cells were transduced with individual types of lentivirus at a multiplicity of infection (MOI) of 10 in the presence of 5 μg/ml puromycin [Hanheng Biotechnology (Shanghai) Co., Ltd.]. The two SKA3 sequence were: shSKA3#1, GATCTGTCTGAT CCTCCTGTT; and shSKA3#2, CCACAGGCAGTGAAC AACTAT. According to the manufacturer's instructions, liver cancer cells were transfected using Block Lentiviral shRNA Expression system (Invitrogen; Thermo Fisher Scientific, Inc.). Subsequent experiments were performed 48 h after transfection.

RNA extraction and reverse transcription-quantitative (RT-q) PCR. Total RNA from cell lines, 11 fresh tissue samples and tissue from athymic nude mice were extracted using TRIzol® reagent (Invitrogen; Thermo Fisher Scientific, Inc.) according to the manufacturer's instruction. The cDNA synthesis was performed according to the manufacturer's instructions (Invitrogen; Thermo Fisher Scientific, Inc.). PCR reaction conditions for all assays were 95°C for 2 min, followed by 40 cycles of amplification (95°C for 10 sec, 60°C for 20 sec and 72°C for 20 sec). RT-qPCR was performed using the following primers: SKA3, forward, 5'-TACACGAGCAAG AAGCCATTAAC-3' and reverse, 5'-GGATACGATGTA CCGCTCAAGT-3'; p21, forward, 5'-CGATGCCAACCT CCTCAACGA-3' and reverse, 5'-TCGCAGACCTCCAGC ATCCA-3'; and Cyclin D1, forward, 5'-AACTACCTGGAC CGCTTCCT-3' and reverse, 5'-CCACTTGAGCTTGTTCCAC CA-3'. GAPDH was used as the endogenous control with the following primers: Forward, 5'-ACAACCTTGGTATCGTGG AAGG-3' and reverse, 5'-GCCATCACGCCACAGTTTC-3'. Expression levels were normalized to those of GAPDH and calculated as $2^{-[(Cq \text{ of genes}) - (Cq \text{ of GAPDH})]}$, where Cq represents the

Table I. Clinicopathological characteristics of patients with hepatocellular carcinoma.

Characteristic	Number of cases
Sex	
Male	99
Female	11
Age, years	
>45	72
≤45	38
Clinical stage	
I	66
II	26
III	12
IV	6
T classification	
T1	52
T2	21
T3	15
T4	22
N classification	
N0	97
N1	13
M classification	
Yes	6
No	104
Cirrhosis	
Yes	67
No	43
Hepatitis B antigen	
Yes	100
No	10
Outcome	
Survival	32
Mortality	78

threshold cycle for each transcript (18). All experiments were repeated three times.

Western blotting. Western blotting was performed as described previously (18). The following antibodies (all 1:1,000) were used: SKA3 (cat. no. ab118560; Abcam), anti-p-Rb (cat. no. D20B12; Cell Signaling Technology, Inc.), anti-Rb (cat. no. D20; Cell Signaling Technology, Inc.) and α -tubulin (cat. no. ab7291; Abcam) as an internal loading control. The expression levels of SKA3 were detected using enhanced chemiluminescence detection system (Amersham; Cytiva) according to the manufacturer's instructions.

Immunohistochemistry (IHC). IHC and SKA3 expression scoring were performed as previously reported (19). Image-Pro Plus version 6.0 software (Media Cybernetics, Inc.) was used to judge the area and density of the dyed region, and the

integrated optical density (IOD) value of the IHC section. The intensity of staining was graded as follows: 0 (no staining), 1 (weak staining, light yellow), 2 (moderate staining, yellow brown), and 3 (strong staining, brown). The proportion of tumor cells was scored as follows: 0 (no positive tumor cells), 1 (<10% positive tumor cells), 2 (10-50% positive tumor cells), 3 (50-75% positive tumor cells), and 4 (>75% positive tumor cells). The staining index (SI) was calculated by the product of the staining intensity score and the proportion of positive tumor cell score. The optimal cut-off value was determined: SI score ≥ 6 was considered to indicate high SKA3 expression, while a score <6 indicated low expression.

Cell proliferation assay. Cell proliferation was measured via MTT assay (Sigma-Aldrich; Merck KGaA). In brief, treated and untreated Huh7 and HepG2 cells were inoculated into 96-well plates. The cells were incubated with 20 μ l 5 mg/ml MTT solution in a humid atmosphere containing 5% CO₂ at 37°C for 4 h. The OD was measured at 490 nm using a spectrophotometer following cell lysis and dissolution of methoxyppyrene in 150 μ l DMSO. The calculation formula of proliferation inhibition rate was as follows: Proliferation inhibition rate = $OD_{\text{sample}}/OD_{\text{control}}$. All experiments were repeated three times, and the mean values were plotted to construct cell proliferation inhibition curves.

Colony formation assay. Both non-transfected and transfected Huh7 and HepG2 cells were seeded in 6-well plates at a density of 1,000 cells/well. After 12 days, cells were fixed with 4% paraformaldehyde for 30 min and stained with 0.1% crystal violet for 30 min at 37°C. Next, the plates were washed gently with PBS, then air dried and the stained colonies were photographed under an inverted light microscope (x200 magnification; Leica Biosystems). The colonies were counted in 10 randomly chosen microscope fields. The experiments were repeated three times.

Cell cycle distribution analysis. Propidium iodide (PI) staining was used to analyze DNA content. Treated and untreated Huh7 and HepG2 cells were washed with PBS and fixed in ice-cold ethanol at -20°C overnight. and stained with staining solution containing 20 μ g/ml PI and 100 μ g/ml RNase (both Sigma-Aldrich; Merck KGaA) for 20 min at 4°C. A FACScan flow cytometer (BD Biosciences) was used to analyze DNA content and FlowJo version 7.6 software (FlowJo LLC) was used to determine the percentage of cells in G₁/G₀, S and G₂/M phase. The experiments were repeated three times.

Luciferase reporter gene assay. Cells were seeded in 24-well plates in triplicate and allowed to stand for 24 h. E2F 3'-untranslated region (UTR) was cloned into the downstream region of the luciferase gene in the pGME2F-Lu luciferase vector. For the reporter assay, the E2F luciferase reporter plasmid pGME2F-Lu Genomeditech Inc.), 1 ng pRL-TK Renilla plasmid (Promega Corporation), and a SKA3 mimic, SKA3 inhibitor or SKA3 control vector were transfected into cells using Lipofectamine 2000 Reagent (Invitrogen; Thermo Fisher Scientific, Inc.). The primer sequences of E2F 5'-3' UTR were 5'-GGCCCGAUCGAUGUUUCCTT-3' (forward) and 5'-GGAAAACAUCGAUCGGGCCTT-3' (reverse). Following

48 h transfection, cells were lysed and luciferase activity was measured using Dual-Luciferase Reporter Assay kit (Promega Corporation) according to the manufacturer's instructions. Data were standardized to *Renilla* luciferase activity.

TCGA data processing and GSEA. In order to investigate the expression levels of SKA3 in liver tissue, data from TCGA (tcgadata.nci.nih.gov/tcga/) was analyzed. Gene expression levels and clinical data of patients were integrated according to their barcode ID. In order to determine the biological pathways underlying the effect of SKA3 in liver cancer, GSEA, a method of using biological knowledge to analyze and interpret microarray and data (20), was conducted using GSEA version 2.0 of the Broad Institute (21). GSEA firstly generated an ordered gene list according to correlation with SKA3 expression, then a pre-defined gene set enrichment score (ES) was obtained to refute the hypothesis that its members are randomly distributed in the ordered list. The BENPORATH_PROLIFERATION gene set (C2. BENPORATH. V3.0) biological process database from the Molecular Signatures Database was used for enrichment analysis (22). P-value was calculated using an arrangement of 1,000 random samples. A false discovery rate (FDR) <25% and nominal P-value <0.05 were considered to indicate a statistically significant difference.

Anchorage-independent growth ability assay. Complete medium agar (1%; Sigma-Aldrich; Merck KGaA) mixture was poured into the wells of a 6-well plate. Following solidification, cells (1×10^3) were digested with trypsin and suspended in 2 ml medium supplemented with 0.3% agar, and then spread on the bottom layer. Following incubating at 37°C, 5% CO₂ for 10 days, colony size was measured with an ocular micrometer and colonies with a diameter >0.1 mm were counted. The experiment was performed independently three times.

Tumor xenograft models. For *in vivo* tumor proliferation assays, a subcutaneous HCC model was established. Twenty six-week-old male BALB/c (nu/nu) mice (average weight, 15 g) were supplied by Beijing Weitong Lihua Laboratory Animal Technology Co., Ltd. The mice were raised in the animal facility at Sun Yat-sen University (Guangzhou, China) under specific pathogen-free laboratory with a 12 h light/dark cycle at 22±2°C and 60±5% humidity, provided with free access to food and water. The mice were randomly divided into four groups (n=5/group) and injected with 2×10⁶ Huh7 cells transfected with empty vector, SKA3, scramble or shSKA3#2. Tumor volume was monitored by measuring the length (L) and width (W) at 3-day intervals for 4 weeks and calculated using the equation $(L \times W^2)/2$. At 4 weeks following liver cancer cell inoculation, all animals were euthanized with 100% CO₂ infused at 30% volume/minute displacement and then subjected to cervical dislocation in accordance with AVMA institutional guidelines (23). Respiratory and cardiac arrest and pupil dilation were considered to indicate animal death. The tumor tissues were dissected, weighed and subjected to pathological examination. The mean animal weight before tumor excision was 21.3±2.2 g. Animal experiments were approved by the Institutional Animal Ethics Committee at Sun Yat-sen University (no. 2017-047).

Statistical analysis. Statistical analysis was performed using SPSS 21.0 (IBM Corp.) statistical software. Each experiment was performed at least in triplicate. All the data are generally expressed as the mean ± SEM or counts and percentages. A chi-square test and Fisher's exact test were used to assess the association between SKA3 expression and clinicopathological factors. Pearson's correlation analysis was used to evaluate the relationship between SKA3 and clinical pathologic factors. The differences between groups were analyzed by two-tailed Student's t-test or one-way ANOVA followed by Tukey's honestly significant difference post hoc test. Survival curves were constructed via the Kaplan-Meier method and compared with log-rank test. Univariate and multivariate Cox regression analysis was used to evaluate the significance of variables for survival. P<0.05 was considered to indicate a statistically significant difference.

Results

SKA3 is upregulated in HCC. SKA3 expression levels were extracted from TCGA liver cancer cohorts and were revealed to be significantly increased in HCC tissue compared with normal liver tissue (Fig. 1A). Furthermore, RT-qPCR was performed to evaluate mRNA expression levels of SKA3 in 10 solid tumor and three normal liver tissue samples from patients. SKA3 mRNA expression levels were significantly elevated in HCC tumors compared with normal tissue (Fig. 1B). SKA3 mRNA levels in all cultured liver cancer cell lines were also significantly higher than those in the normal hepatocyte lines (Fig. 1C). In order to investigate whether SKA3 was also upregulated at the protein level, western blotting was performed. The protein levels of SKA3 in clinical HCC tissue and cultured liver cancer cell lines were upregulated compared with their normal counterparts (Fig. 1D and E). These results indicated that SKA3 is overexpressed in HCC at both the mRNA and protein level.

Association between SKA3 expression levels and clinical features of HCC. In order to determine the clinical significance of SKA3 in liver cancer, the expression levels of SKA3 were studied in 110 paraffin-embedded liver cancer tissue samples using IHC analysis. Samples including 66 cases of stage I, 26 cases of stage II, 12 cases of stage III and 6 cases of stage IV tumor (Table I). As shown in Table II, SKA3 was positively expressed in 105 samples (95.5%), with high expression in 59 samples (53.6%) and low expression in 51 samples (46.4%). Correlations between SKA3 expression levels and clinicopathological characteristics of HCC were evaluated using Chi-square test and Pearson's correlation analysis (Tables III and IV). Kaplan-Meier survival analysis and log-rank test were used to evaluate the association between SKA3 expression levels and prognosis. Survival status of patients with high and low expression levels of SKA3 was analyzed (Fig. 2A). The overall survival time of patients with HCC with high levels of SKA3 was shorter than those of patients with low levels of SKA3 (Fig. 2B; log-rank P-value=0.002). Univariate and multivariate Cox regression analysis demonstrated that SKA3 expression and clinical stage were independent prognostic factors for patients with HCC (Table V).

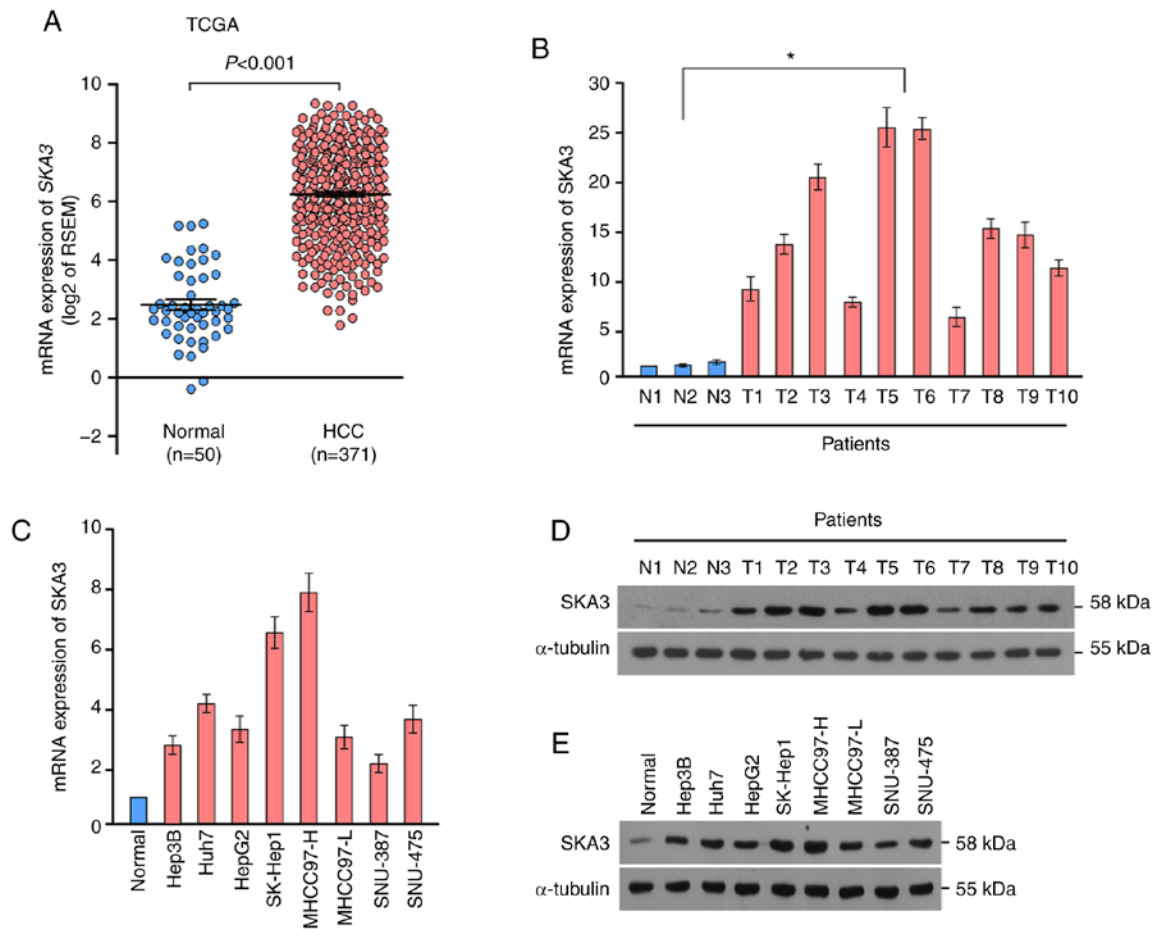


Figure 1. SKA3 is upregulated in liver cancer tissue and cells. (A) mRNA expression levels of SKA3 are upregulated in tumor tissue compared with normal tissue in The Cancer Genome Atlas liver cancer cohort. mRNA expression of SKA3 is upregulated in (B) tumor tissue and (C) cultured liver cancer cell lines. SKA3 protein expression levels in (D) tumor tissue and (E) cultured liver cancer cell lines were examined by western blotting. Data are presented as the mean \pm SEM (n=3). *P<0.05. SKA3, spindle and kinetochore associated complex subunit 3; RSEM, RNA-Seq by Expectation-Maximization; N, normal; T, tumor.

SKA3 promotes proliferation of liver cancer cells. In order to study the potential signaling pathways that contribute to SKA3-mediated proliferation of liver cancer cells, GSEA was used to identify associated signaling pathways. Gene expression level profiles of patients with low and high expression of SKA3 in the TCGA HCC cohort (371 patients, divided by the median expression of SKA3 mRNA) were compared. In the BENPORATH_PROLIFERATION gene set, the proliferation pathway was significantly enriched in the SKA3_High group (Fig. 3A). In order to evaluate the function of SKA3 *in vitro*, Huh7 and HepG2 cells were transfected with SKA3-expressing lentivirus to overexpress SKA3, or shRNA to silence SKA3. The efficiency of the overexpression and knockdown of SKA3 expression was examined by western blotting (Fig. 3B). In addition, in order to explore the association between the expression of SKA3 and the proliferation ability of HCC cells, MTT assay was performed. Knockdown of SKA3 significantly decreased the proliferation rate, and overexpression of SKA3 resulted in increased proliferation compared with the corresponding control liver cancer cell lines, both in Huh7 and HepG2 cells (Fig. 3C). The results demonstrated that SKA3 affected the proliferation of liver cancer cells. Colony formation assays were performed to evaluate the colony formation function of SKA3 *in vitro*, which demonstrated that silencing SKA3 colony formation, whereas overexpression of SKA3 increased colony formation (Fig. 3D).

SKA3 promotes cell cycle progression. Flow cytometry analysis was performed to determine whether the effect of SKA3 on the proliferation of liver cancer cells was affected by cell cycle arrest. The results showed that shRNA-transfected liver cancer cells were arrested at the G₁/G₀ phase and the percentage of cells in S-phase decreased, whereas in cells transfected with SKA3-expressing lentivirus, the percentage of cells in S-phase increased (Fig. 4A). GSEA analysis showed that high expression of SKA3 was associated with E2F1 and its target genes (Fig. 4B). Luciferase reporter activity assay revealed that the luciferase activity of the wild-type E2F-regulated 3'UTR was significantly upregulated by 6.5-fold, whereas knockdown of SKA3 significantly inhibited luciferase activity by 80% in Huh7 and HepG2 cells (Fig. 4C). Protein p21 inhibits the activity of the cyclin D1 complex, which results in decreased phosphorylation of Rb, in turn inhibiting the release of E2F1 from the Rb-E2F1 inhibitory complex, followed by enhanced expression of E2F1 target genes (24). In order to investigate whether mRNA and protein levels of associated cell cycle regulatory oncogenes are also upregulated in liver cancer cell lines with overexpressed and silenced SKA3, RT-qPCR and western blot analysis were performed. RT-qPCR demonstrated significant upregulation of p21 and downregulation of cyclin D1 in Huh7 and HepG2 cells overexpressing SKA3 (Fig. 4D).

Table II. Expression levels of SKA3 in hepatocellular carcinoma.

Expression of SKA3	Number of cases (%)
Negative	5 (4.5)
Positive	105 (95.5)
Low	51 (46.4)
High	59 (53.6)
SKA3, spindle and kinetochore associated complex subunit 3.	

Table III. Correlation between SKA3 expression levels and clinicopathological characteristics of hepatocellular carcinoma.

Characteristic	SKA3		Chi-square test P-value	Fisher's Exact test P-value
	Low	High		
Sex			0.566	0.752
Male	45	54		
Female	6	5		
Age, years			0.878	1.000
>45	33	39		
≤45	18	20		
Clinical stage			0.084	0.121
I/II	46	46		
III/IV	5	13		
T classification			0.013 ^a	0.016 ^a
T1/2	40	33		
T3/4	11	26		
N classification			0.073	0.084
N0	48	49		
N1	3	10		
M classification			0.134	0.213
No	50	54		
Yes	1	5		
Cirrhosis			0.230	0.246
Yes	28	39		
No	23	20		
Hepatitis B antigen			0.809	1.000
Yes	46	54		
No	5	5		
Outcome			0.009 ^a	0.012 ^a
Survival	21	11		
Mortality	30	48		

SKA3, spindle and kinetochore associated complex subunit 3;
^aP<0.05 indicates statistical significance.

Table IV. Pearson's correlation analysis between SKA3 and clinicopathological factors.

Variable	SKA3 expression levels	
	Pearson correlation	P-value
Sex	0.055	0.570
Age	0.015	0.879
Clinical stage	0.165	0.085
T classification	0.237	0.012 ^a
N classification	0.171	0.074
M classification	0.143	0.136
Cirrhosis	0.114	0.234
Hepatitis B antigen	0.023	0.811
Outcome	0.247	0.009 ^a

^aP<0.05 indicates statistical significance.

SKA3 and downregulated in liver cancer cells transfected with shSKA3, whereas levels of p21 were downregulated in liver cancer cells transfected with SKA3 and elevated in liver cancer cells transfected with shSKA3 (Fig. 4E). These results demonstrated that expression of SKA3 facilitated cell cycle progression in liver cancer cells.

SKA3 promotes tumorigenesis of HCC cells. In order to examine the effects of SKA3 on the growth of liver cancer cells, the anchorage-independent growth assay was performed. Quantitation of the number of spheres formed over serial passages showed that overexpression of SKA3 significantly increased sphere formation, whereas knockdown of SKA3 by transfection with shSKA3 significantly inhibited the sphere formation ability of Huh7 and HepG2 cell lines (Fig. 5A). In order to examine the effects of SKA3 on liver cancer cell growth *in vivo*, a subcutaneous tumor xenograft model was established. In athymic nude mice injected subcutaneously with Huh7 cells transfected with SKA3, the tumor volume and weight increased significantly, whereas in those injected with cells transfected with shSKA3, they decreased significantly (Fig. 5B-D). Differences in SKA3 expression levels in tumor tissue of each group were investigated by IHC, which demonstrated that SKA3 expression levels significantly increased in the group injected subcutaneously with Huh7 cells transfected with SKA3 (Fig. 5E). Furthermore, to explore whether associated cell cycle regulatory oncogenes were also upregulated in liver cancer tissue from these mice, mRNA and protein were extracted and RT-qPCR and western blotting were performed. RT-qPCR revealed significant downregulation of p21 and upregulation of cyclin D1 in the SKA3-overexpression HCC tissue group (Fig. S1). Western blotting revealed that the levels of cyclin D1 and p-Rb were elevated in the SKA3-overexpression and downregulated in shSKA3 HCC tissue group, while the levels of p21 were downregulated in liver cancer cells transfected with SKA3 and elevated in liver cancer cells transfected with shSKA3 (Fig. 5F). These results demonstrated that the expression of SKA3 increased liver tumor cell growth both *in vivo* and *in vitro*.

Western blotting revealed that the levels of cyclin D1 and p-Rb were elevated in liver cancer cells transfected with

Table V. Univariate and multivariate Cox regression analysis of prognostic parameters in patients with hepatocellular carcinoma.

Parameter	Univariate analysis			Multivariate analysis		
	Number of patients	P-value	Regression coefficient (SEM)	P-value	Relative risk	95% CI
Clinical stage						
I/II	92	<0.001	1.307 (0.284)	<0.001	3.120	1.766-5.512
III/IV	18					
Expression of SKA3						
Low	51	0.003	0.708 (0.234)	0.023	1.733	1.079-2.781
High	59					

SKA3, spindle and kinetochore associated complex subunit 3.

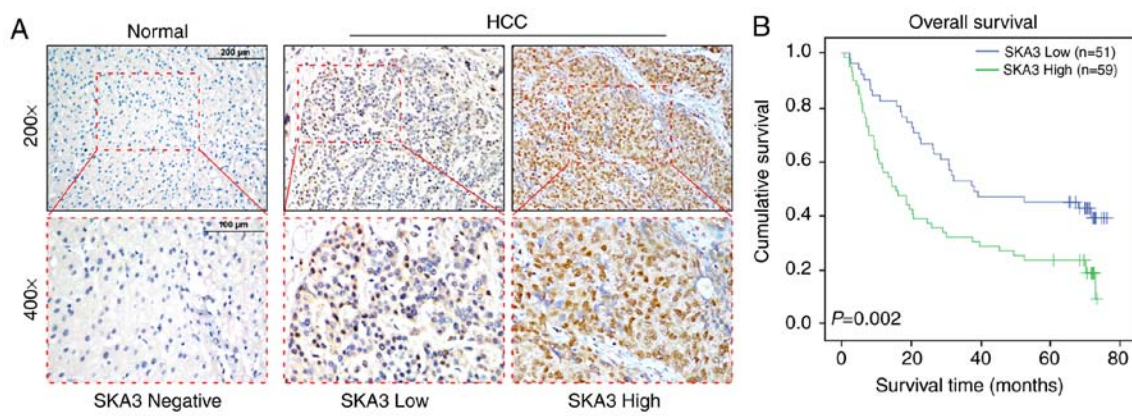


Figure 2. Expression levels of SKA3 in patients with HCC. (A) Representative images from immunohistochemistry analysis of SKA3 expression levels in normal liver and low and high SKA3 HCC tissue. (B) Kaplan-Meier analysis of overall survival in patients with HCC with low (n=51) vs. high SKA3 expression (n=59). SKA3, spindle and kinetochore associated complex subunit 3; HCC, hepatocellular carcinoma.

Discussion

The present study found that knockdown of SKA3, which was highly expressed in TCGA HCC cohorts, inhibited the tumorigenicity and proliferation of liver cancer cells both *in vivo* and *in vitro*. Silencing SKA3 with shRNA inhibited E2F activity, which led to upregulation of CDK inhibitor p21 and the downregulation of CDK regulatory protein cyclin D1. Overexpression of SKA3 had the opposite effects. These results indicated that upregulation of SKA3 served an important role in promoting tumorigenesis and progression of liver cancer.

Tumorigenesis is characterized by uncontrolled tumor formation and cell growth, and is associated with alterations in genes or proteins involved in regulation of proliferation and genomic instability (25). Therefore, identification of genes and their products associated with the molecular events leading to tumorigenesis is essential for formulating effective therapeutic strategies. The present study reported that SKA3 was markedly upregulated in liver cancer cells/clinical tissue compared with normal liver cells/non-cancerous tissue at both the transcriptional and translational levels. Statistical analysis of IHC staining revealed that the expression levels of SKA3 were significantly correlated with clinicopathological characteristics and patient survival. Furthermore, shRNA

silencing of SKA3 decreased the tumorigenicity of liver cancer cells both *in vivo* and *in vitro*, suggesting that SKA3 may serve an oncogenic role in the development and progression of liver cancer.

Lee *et al* (13) reported that SKA3 mRNA is upregulated in prostate cancer cells and tissue. Similarly, SKA3 overexpression has also been implicated in colorectal cancer (11,12). Chuang *et al* (11) suggested that SKA3 at 13q12.11 may be a novel gene involved in malignant transformation of colorectal cancer. SKA3 is a subunit located in the outer layer of the SKA complex, which can control and promote proper exit during mitosis together with the NDC80 kinetochore complex component (26,27). When spindle checkpoints are silenced by checkpoint kinase inhibition, or when cells are forced to exit mitosis by CDK1 inactivation downstream of checkpoint silencing, SKA3-deficient cells exhibit slower mitotic exit. Mitotic arrest is induced by SKA3 depletion in HeLa cells (6,7). To the best of our knowledge, however, the oncogenic ability of SKA3 has not been studied in liver cancer. Here, SKA3 depletion in Huh7 and HepG2 cells significantly decreased cell growth, cell cycle arrest, colony formation and proliferation ability. These results suggested that SKA3 served an important role in mitotic checkpoints in liver cancer cells.

In order to determine the potential mechanism involved in SKA3-mediated enhancement of liver cancer cell aggression,

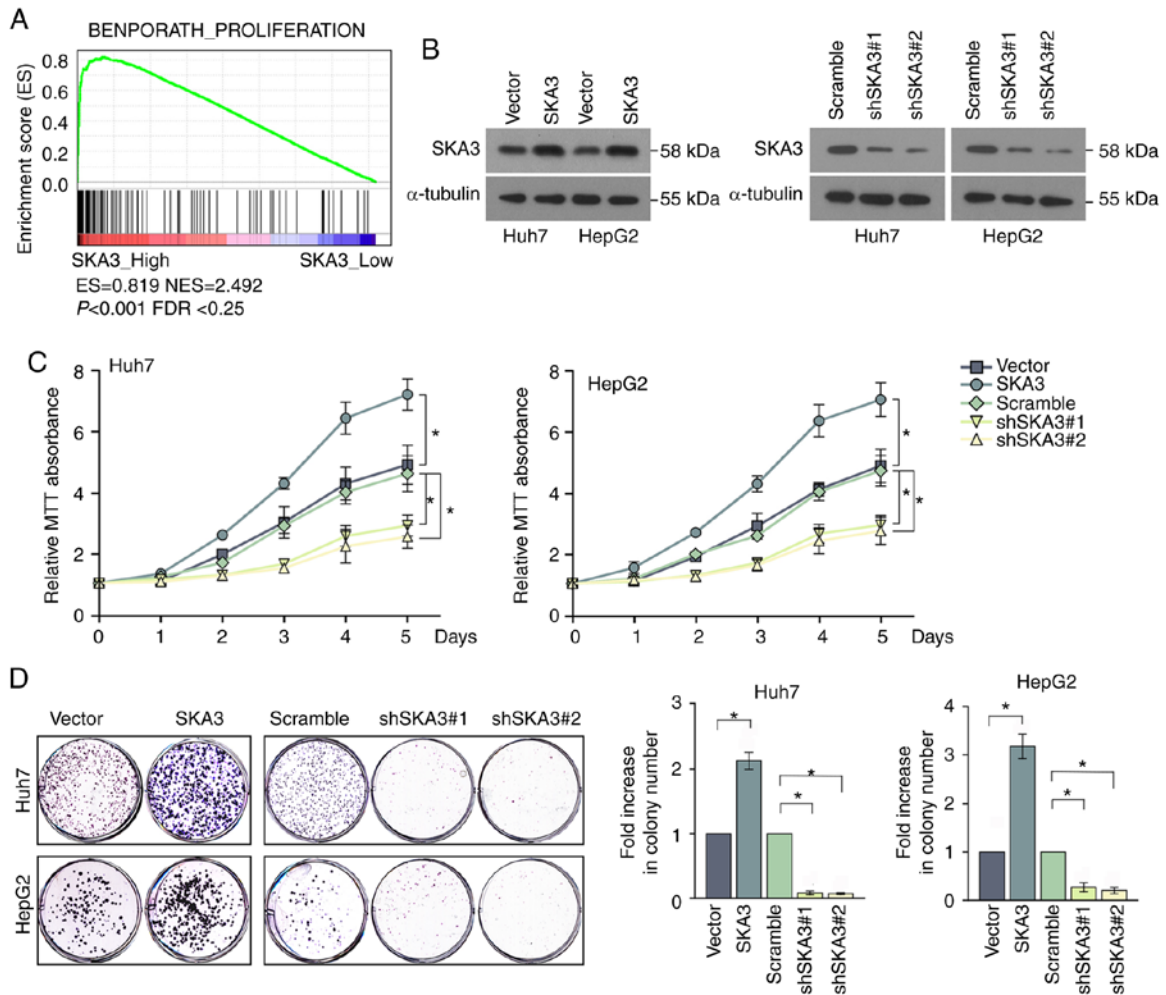


Figure 3. SKA3 increases proliferation in liver cancer cell lines. (A) Gene sets enrichment analysis delineating the signaling pathways of proliferation associated with SKA3 expression in the liver cancer cohort. (B) Overexpression and knockdown of SKA3 in two specific shRNA-transduced stable liver cancer cell lines. (C) Knockdown of SKA3 inhibited the cell proliferation rate, as determined by MTT assay. (D) Colony formation assay using untreated and treated liver cancer cells (left). Quantification of the colony number is shown (right). Data are presented as the mean \pm SEM ($n=3$). * $P<0.05$. SKA3, spindle and kinetochore associated complex subunit 3; sh, short hairpin; ES, enrichment score; NES, normalized enrichment score.

GSEA was performed to identify signaling pathways associated with SKA3 expression using high throughput RNA-sequencing data of the HCC cohort of TCGA. Uncontrolled progression through G_1/S and G_2/M cell cycle transition can lead to uncontrolled cell proliferation and cancer (28). Hou *et al* (29) showed that G_2/M phase arrest is caused by SKA3 knockdown resulting in inhibited CDK2/p53 phosphorylation in HCC cells. However, the present results showed that when SKA3 increased relative to vector-alone, the number of Huh7 cells in G_2/M decreased but there was no significant change in numbers of HepG2 cells. This may be because Huh7 contains p53 mutant and HepG2 contains wild-type p53 (30). p53 suppresses the expression of CDK1 and cyclins B1 and D1, resulting in cell cycle (G_2/M) arrest (or delay) (31). SKA3 may affect cell cycle (G_2/M) by inhibiting transcriptional activation of p53 in Huh7 cells. Furthermore, wild-type p53 triggered the opposite effect and blocked the effect of SKA3 on cell cycle progression in HepG2 cells, resulting in a smaller proportion of HepG2 cells transfected with vector at G_2/M phase than that of Huh7 cells transfected with vector, which covered the effect of SKA3 on G_2/M phase in HepG2 cells transfected with SKA3 or shSKA3.

Transcription factor E2F1 is a key cell cycle regulator. Its target genes encode proteins that regulate cell cycle progression through G_1/S transition and serve an important role in DNA repair and apoptosis (32). Gene set enrichment analysis demonstrated that E2F1 gene expression was significantly different between the SKA3-high and -low groups. The E2F transcription factor family plays a key role in cell cycle progression (33). E2F1 is part of the E2F protein family, which can promote or inhibit breast cancer cell proliferation and serves a role in DNA replication (34,35), DNA damage checkpoint control and apoptosis (36). Luciferase reporter activity assay revealed that overexpression of SKA3 significantly increased the luciferase activity of E2F-regulated transcripts. Increased DNA replication may be caused by promotion of E2F activity and expression by p-Rb, suggesting a potential route to SKA3-associated tumorigenesis and cell cycle progression. Downregulation of cyclin D1 and upregulation of p21 may be a promising therapeutic strategy to suppress growth of cancer cells (37,38). Expression of oncogenes inhibits p21, activates cyclin D1-CDK4 and specifically phosphorylates Rb in G_1 phase, resulting in the release of E2F1 from the Rb-E2F1 inhibitory complex, and ultimately facilitates G_1 to S phase transition (24,39,40). Hu *et al* (41) demonstrated

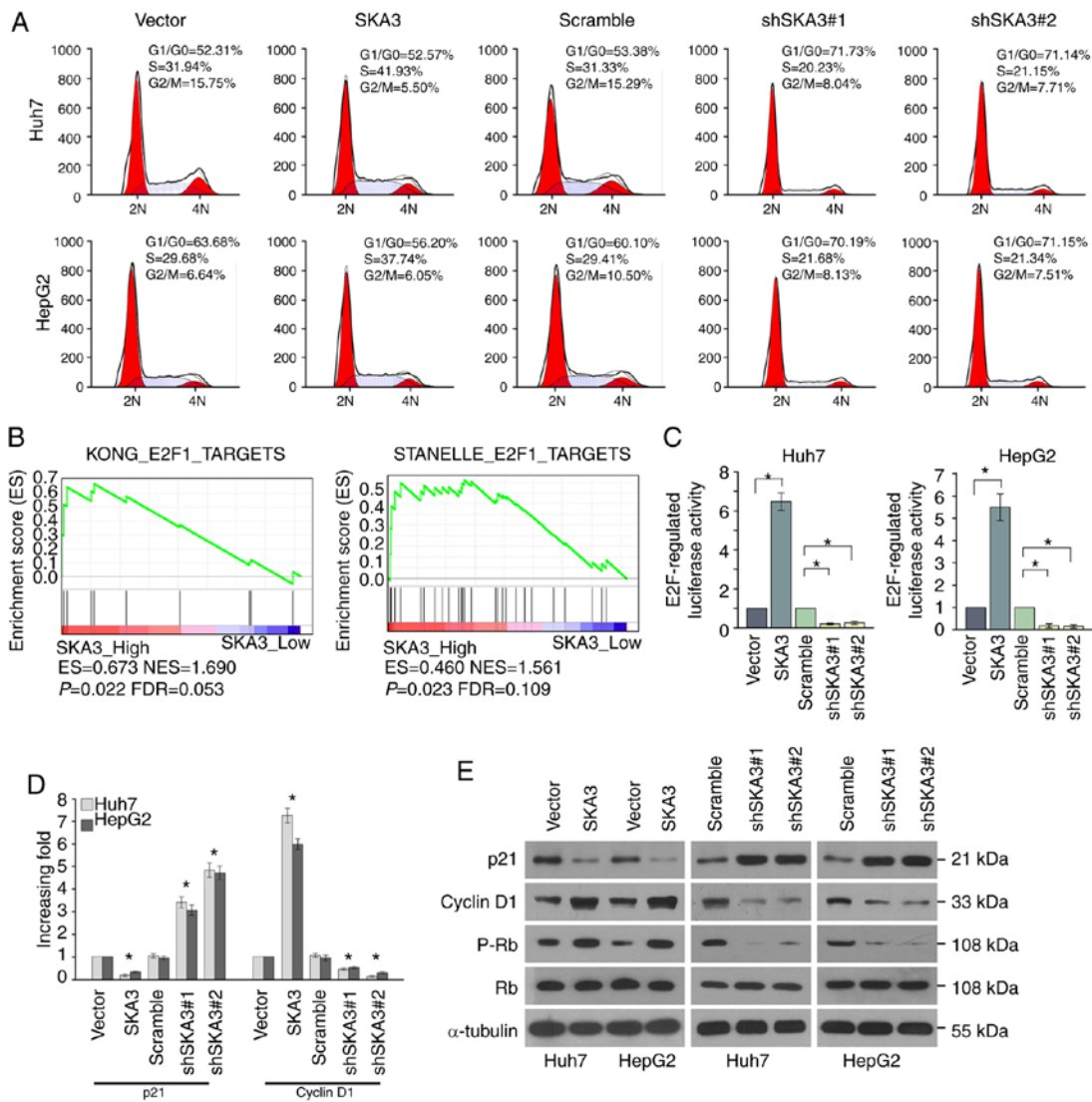


Figure 4. Depletion of SKA3 induces G₁/S arrest of liver cancer cells. (A) Cell cycle distribution analysis of liver cancer cells transfected with vector or each of the two SKA3 shRNAs. (B) Gene sets enrichment analysis showing that the E2F1 target gene was associated with SKA3 expression levels. (C) Luciferase reporter gene assay showing that overexpression of SKA3 significantly increased luciferase activity of E2F-regulated cells. (D) Relative mRNA expression levels of p21 and cyclin D1 were determined by reverse transcription-quantitative PCR. (E) Western blotting analysis of p21, cyclin D1, Rb and p-Rb. Data are presented as the mean \pm SEM (n=3). *P<0.05. SKA3, spindle and kinetochore associated complex subunit 3; sh, short hairpin; Rb, retinoblastoma; p, phosphorylated; ES, enrichment score; NES, normalized enrichment score.

that SKA3 is involved in regulating cell cycle progression and increased levels of p-AKT, cyclin E2, CDK2, cyclin D1, CDK4, E2F1 and p-Rb in HeLa cells. Western blotting and RT-qPCR analysis here revealed that the overexpression of SKA3 suppressed expression levels of p21, and elevated those of cyclin D1, E2F1 and p-Rb in liver cancer cells transfected with SKA3.

Cancer development and progression is a multi-step process. Gene mutation and alteration in gene transcription and translation may be specific biomarkers for cancer (19). In-depth understanding of the molecular mechanism underlying liver cancer pathogenesis, especially genetic alterations in liver cancer, may provide novel insights for the diagnosis and treatment of liver cancer, thereby improving clinical efficacy. In the present study, SKA3 was significantly associated with aggressive features and unfavorable clinicopathological characteristics of liver cancer. Compared with patients with low expression levels of SKA3, the overall survival time of patients with

high expression levels of SKA3 was significantly decreased. Furthermore, Cox regression analysis showed that SKA3 and clinical stage may be independent risk factors for patients with HCC. The present study also demonstrated that SKA3 was associated with the aggressiveness of liver cancer and may serve as a useful prognostic marker for patients with liver cancer.

The present study showed that SKA3 was upregulated in liver cancer tissue and cell lines, and its high expression was associated with poor prognosis of liver cancer. Knockdown of SKA3 may suppress tumor growth by inducing arrest at the G₁/S phase and inhibiting proliferation of liver cancer cells. The inhibitory effect of SKA3 knockdown was further confirmed by *in vivo* assays. The present study demonstrated that SKA3 may be a diagnostic and prognostic marker for patients with liver cancer. The expression levels of SKA3 were associated with survival of patients with liver cancer. Therefore, inhibiting expression of SKA3 may provide an effective therapeutic strategy in liver cancer.

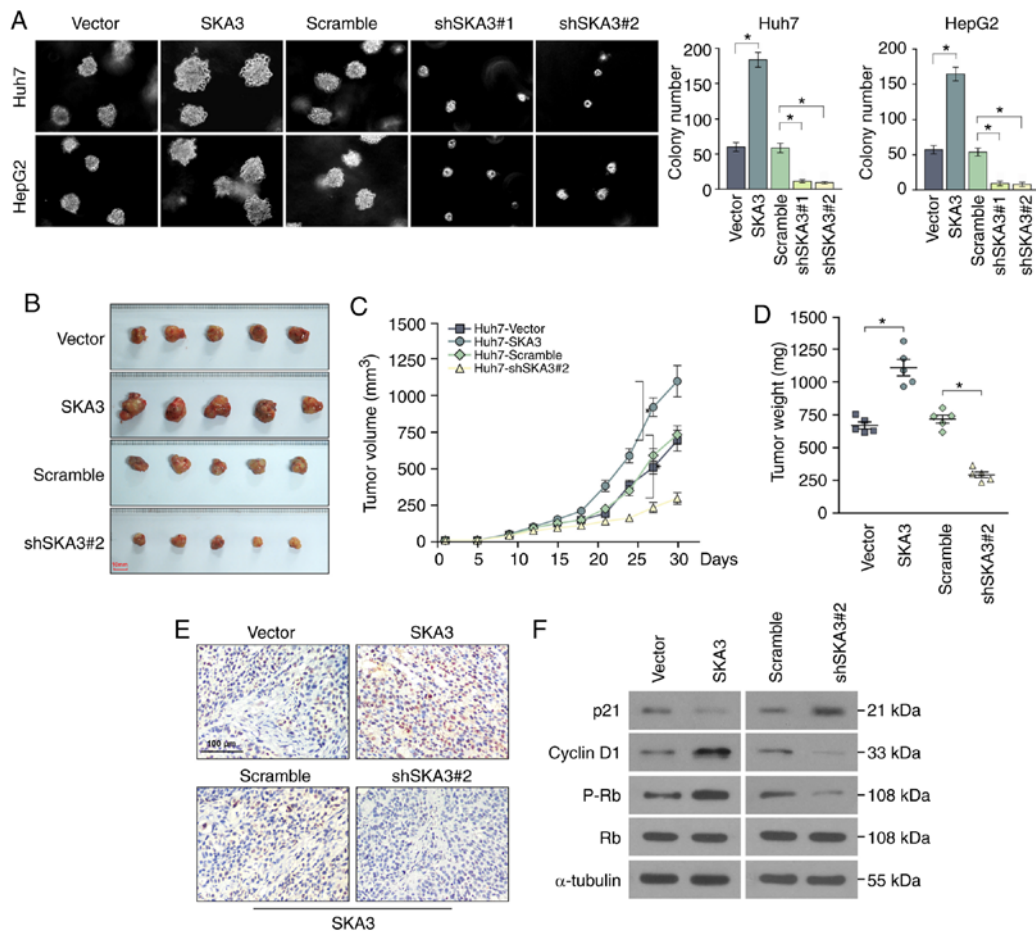


Figure 5. Knockdown of SKA3 inhibits tumorigenicity of liver cancer cells *in vitro* and *in vivo*. (A) Silencing SKA3 inhibited cell growth, as determined by anchorage-independent growth assay following 10 days of culture (left). Colonies containing >50 cells were scored (right). (B) Representative images of tumors from a xenograft model using nude mice injected subcutaneously with Huh7 cells transfected with empty vector, SKA3, scramble or shSKA3#2. (C) Tumor volume was measured on the indicated days. (D) Tumor weight was measured at 4 weeks post-injection. (E) Representative images from immunohistochemistry analysis of SKA3 expression levels in mouse tumor tissue. (F) Western blotting analysis of p21, cyclin D1, Rb and p-Rb protein expression levels in mouse tumor tissue derived from xenograft model at 4 weeks post-injection. Data are presented as the mean \pm SEM (n=3). *P<0.05. SKA3, spindle and kinetochore associated complex subunit 3; sh, short hairpin; Rb, retinoblastoma; p, phosphorylated.

Acknowledgements

The authors would like to thank Professor Weixia Zeng from Sun Yat-sen University Cancer Center (Guangzhou, China) for reviewing the manuscript.

Funding

The present study was supported by the National Natural Science Foundation of China (grant nos. 81871999 and 81572368), Guangdong Natural Science Foundation (grant no. 2016A030313278), Science and Technology Planning Project of Guangdong Province, China (grant no. 2014A020212084), and Shenzhen Key Medical Discipline Construction Fund (SZXK079). The funders had no role in study design, data collection, analysis and interpretation, or preparation of the manuscript.

Availability of data and materials

The datasets used and/or analyzed during the current study are available from the corresponding author on reasonable request.

Authors' contributions

JT performed cell culture experiments, collected and analyzed data and drafted the manuscript. JLi and JLi performed cell culture experiments and drafted the manuscript. ZL performed and interpreted the array GSEA data. HL and KZ performed western blotting, immunohistochemistry and quantitative PCR analysis. ZZ conceptualized the study. NJ and LZ conceptualized the study and drafted the manuscript. All authors read and approved the final manuscript.

Ethics approval and consent to participate

The present study was approved by the Clinical Research Ethics Committee of the Third Affiliated Hospital of Sun Yat-sen University. Informed written consent was obtained from all patients.

Patient consent for publication

Not applicable.

Competing interests

The authors declare that they have no competing interests.

References

- El-Serag HB and Rudolph KL: Hepatocellular carcinoma. Epidemiology and molecular carcinogenesis. *Gastroenterology* 132: 2557-2576, 2007.
- Torre LA, Bray F, Siegel RL, Ferlay J, Lortet-Tieulent J and Jemal A: Global cancer statistics, 2012. *CA Cancer J Clin* 65: 87-108, 2015.
- Zhang S, Yue M, Shu R, Cheng H and Hu P: Recent advances in the management of hepatocellular carcinoma. *J BUON* 21: 307-311, 2016.
- Vibert E, Schwartz M and Olthoff KM: Advances in resection and transplantation for hepatocellular carcinoma. *J Hepatol* 72: 262-276, 2020.
- Lei X, Xu JF, Chang RM, Fang F, Zuo CH and Yang LY: JARID2 promotes invasion and metastasis of hepatocellular carcinoma by facilitating epithelial-mesenchymal transition through PTEN/AKT signaling. *Oncotarget* 7: 40266-40284, 2016.
- Sivakumar S and Gorbsky GJ: Phosphatase-regulated recruitment of the spindle- and kinetochore-associated (Ska) complex to kinetochores. *Biol Open* 6: 1672-1679, 2017.
- Abad MA, Zou J, Medina-Pritchard B, Nigg EA, Rappsilber J, Santamaria A and Jeyaprakash AA: Ska3 ensures timely mitotic progression by interacting directly with microtubules and skai1 microtubule binding domain. *Sci Rep* 6: 34042, 2016.
- Raaijmakers JA, Tanenbaum ME, Maia AF and Medema RH: RAMA1 is a novel kinetochore protein involved in kinetochore-microtubule attachment. *J Cell Sci* 122: 2436-2445, 2009.
- Ohta S, Bukowski-Wills JC, Sanchez-Pulido L, de Lima Alves F, Wood L, Chen ZA, Platani M, Fischer L, Hudson DF, Ponting CP, *et al*: The protein composition of mitotic chromosomes determined using multiclassifier combinatorial proteomics. *Cell* 142: 810-821, 2010.
- Zhang Q, Sivakumar S, Chen Y, Gao H, Yang L, Yuan Z, Yu H and Liu H: Ska3 phosphorylated by Cdk1 binds Ndc80 and recruits ska to kinetochores to promote mitotic progression. *Curr Biol* 27: 1477-1484, 2017.
- Chuang TP, Wang JY, Jao SW, Wu CC, Chen JH, Hsiao KH, Lin CY, Chen SH, Su SY, Chen YJ, *et al*: Over-Expression of AURKA, SKA3 and DSN1 contributes to colorectal adenoma to carcinoma progression. *Oncotarget* 7: 45803-45818, 2016.
- Pesson M, Volant A, Uguen A, Trillet K, De La Grange P, Aubry M, Daoulas M, Robaszekiewicz M, Le Gac G, Morel A, *et al*: A gene expression and pre-mRNA splicing signature that marks the adenoma-adenocarcinoma progression in colorectal cancer. *PLoS One* 9: e87761, 2014.
- Lee M, Williams KA, Hu Y, Andreas J, Patel SJ, Zhang S and Crawford NP: GNL3 and SKA3 are novel prostate cancer metastasis susceptibility genes. *Clin Exp Metastasis* 32: 769-782, 2015.
- Tang D, Zhao X, Zhang L, Wang Z and Wang C: Identification of hub genes to regulate breast cancer metastasis to brain by bioinformatics analyses. *J Cell Biochem* 120: 9522-9531, 2019.
- Amin MB, Greene FL, Edge SB, Compton CC, Gershenwald JE, Brookland RK, Brookland RK, Meyer L, Gress DM, Byrd DR and Winchester DP: The eighth edition AJCC cancer staging manual: Continuing to build a bridge from a population-based to a more 'personalized' approach to cancer staging. *CA Cancer J Clin* 67: 93-99, 2017.
- Lecluyse EL and Alexandre E: Isolation and culture of primary hepatocytes from resected human liver tissue. *Methods Mol Biol* 640: 57-82, 2010.
- Vondran FW, Katenz E, Schwartlander R, Morgul MH, Raschok N, Gong X, Cheng X, Kehr D and Sauer IM: Isolation of primary human hepatocytes after partial hepatectomy: Criteria for identification of the most promising liver specimen. *Artif Organs* 32: 205-213, 2008.
- Livak KJ and Schmittgen TD: Analysis of relative gene expression data using real-time quantitative PCR and the 2(-Delta Delta C(T)) method. *Methods* 25: 402-408, 2001.
- Chen SP, Zhang LS, Fu BS, Zeng XC, Yi HM and Jiang N: Prostate tumor overexpressed 1 is a novel prognostic marker for hepatocellular carcinoma progression and overall patient survival. *Medicine (Baltimore)* 94: e423, 2015.
- Debrabant B: The null hypothesis of GSEA, and a novel statistical model for competitive gene set analysis. *Bioinformatics* 33: 1271-1277, 2017.
- Tsuzuki S and Seto M: Expansion of functionally defined mouse hematopoietic stem and progenitor cells by a short isoform of RUNX1/AML1. *Blood* 119: 727-735, 2012.
- Ben-Porath I, Thomson MW, Carey VJ, Ge R, Bell GW, Regev A and Weinberg RA: An embryonic stem cell-like gene expression signature in poorly differentiated aggressive human tumors. *Nat Genet* 40: 499-507, 2008.
- Shomer NH, Allen-Worthington KH, Hickman DL, Jonnalagadda M, Newsome JT, Slate AR, Valentine H, Valentine H and Wilkinson M: Review of rodent euthanasia methods. *J Am Assoc Lab Anim Sci* 59: 242-253, 2020.
- Chen S, Zhou Q, Guo ZN, Wang Y, Wang L, Liu X, Lu M, Ju L, Xiao Y and Wang X: Inhibition of MELK produces potential anti-tumour effects in bladder cancer by inducing G1/S cell cycle arrest via the ATM/CHK2/p53 pathway. *J Cell Mol Med* 24: 1804-1821, 2019.
- Doerfler W, Hohlweg U, Müller K, Remus R, Heller H and Hertz J: Foreign DNA integration--perturbations of the genome--oncogenesis. *Ann N Y Acad Sci* 945: 276-288, 2001.
- Helgeson LA, Zelter A, Riffle M, MacCoss MJ, Asbury CL and Davis TN: The human ska complex and Ndc80 complex interact to form a load-bearing assembly that strengthens kinetochore-microtubule attachments. *Proc Natl Acad Sci USA* 115: 2740-2745, 2018.
- Sivakumar S, Daum JR, Tipton AR, Rankin S and Gorbsky GJ: The spindle and kinetochore-associated (Ska) complex enhances binding of the anaphase-promoting complex/cyclosome (APC/C) to chromosomes and promotes mitotic exit. *Mol Biol Cell* 25: 594-605, 2014.
- Shi Y, Guo S, Wang Y, Liu X, Li Q and Li T: Lamprey prohibitin2 arrest G2/M phase transition of heLa cells through down-regulating expression and phosphorylation level of cell cycle proteins. *Sci Rep* 8: 1-8, 2018.
- Hou Y, Wang Z, Huang S, Sun C, Zhao J, Shi J, Li Z, Wang Z, He X, Tam NL and Wu L: SKA3 Promotes tumor growth by regulating CDK2/P53 phosphorylation in hepatocellular carcinoma. *Cell Death Dis* 10: 929, 2019.
- Kanno S, Kurauchi K, Tomizawa A, Yomogida S and Ishikawa M: Pifithrin-Alpha has a p53-independent cytoprotective effect on docosahexaenoic acid-induced cytotoxicity in human hepatocellular carcinoma HepG2 cells. *Toxicol Lett* 232: 393-402, 2015.
- Liu L, Zhang P, Bai M, He L, Zhang L, Liu T, Yang Z, Duan M, Liu M, Liu B, *et al*: P53 Upregulated by HIF-1 α promotes hypoxia-induced G2/M arrest and renal fibrosis in vitro and in vivo. *J Mol Cell Biol* 11: 371-382, 2019.
- Lynn AS: Inhibition of E2F1 activity and cell cycle progression by arsenic via retinoblastoma protein. *Cell Cycle* 16: 2058-2072, 2017.
- Wang L, Chen H, Wang C, Hu Z and Yan S: Negative regulator of E2F transcription factors links cell cycle checkpoint and DNA damage repair. *Proc Natl Acad Sci USA* 115: E3837-E3845, 2018.
- Mori K, Uchida T, Fukumura M, Tamiya S, Higurashi M, Sakai H, Ishikawa F and Shibamura M: Linkage of E2F1 transcriptional network and cell proliferation with respiratory chain activity in breast cancer cells. *Cancer Sci* 107: 963-971, 2016.
- Nikolai BC, Lanz RB, York B, Dasgupta S, Mitsiades N, Creighton CJ, Tsimelzon A, Hilsenbeck SG, Lonard DM, Smith CL and O'Malley BW: HER2 signaling drives DNA anabolism and proliferation through SRC-3 phosphorylation and E2F1-regulated genes. *Cancer Res* 76: 1463-1475, 2016.
- Cataldo A, Cheung DG, Balsari A, Tagliabue E, Coppola V, Iorio MV, Palmieri D and Croce CM: MiR-302b enhances breast cancer cell sensitivity to cisplatin by regulating E2F1 and the cellular DNA damage response. *Oncotarget* 7: 786-797, 2016.
- Sheldon LA: Inhibition of E2F1 activity and cell cycle progression by arsenic via retinoblastoma protein. *Cell Cycle* 16: 2058-2072, 2017.
- Takahashi Y, Rayman JB and Dynlacht BD: Analysis of promoter binding by the E2F and pRB families in vivo: Distinct E2F proteins mediate activation and repression. *Genes Dev* 14: 804-816, 2000.
- Datta D, Anbarasu K, Rajabather S, Priya RS, Desai P and Mahalingam S: Nucleolar GTP-binding protein-1 (NGP-1) promotes G1 to S phase transition by activating cyclin-dependent kinase inhibitor p21 Cipl/Waf1. *J Biol Chem* 290: 21536-21552, 2015.
- Chang MM, Lai MS, Hong SY, Pan BS, Huang H, Yang SH, Wu CC, Sun HS, Chuang JI, Wang CY and Huang BM: FGF9/FGFR2 increase cell proliferation by activating ERK1/2, Rb/E2F1, and cell cycle pathways in mouse leydig tumor cells. *Cancer Sci* 109: 3503-3518, 2018.
- Hu R, Wang MQ, Niu WB, Wang YJ, Liu YY, Liu LY, Wang M, Zhong J, You HY, Wu XH, *et al*: SKA3 promotes cell proliferation and migration in cervical cancer by activating the PI3K/Akt signaling pathway. *Cancer Cell Int* 18: 183, 2018.